DOI: 10.1111/mice.12593

ORIGINAL ARTICLE

COMPUTER-AIDED CIVIL AND INFRASTRUCTURE ENGINEERING WILEY

Drone scheduling for construction site surveillance

Wen Yi | **Monty Sutrisna**

School of Built Environment, College of Sciences, Massey University, Auckland, New Zealand

Correspondence
Wen Yi, School of Built Environment, College of Sciences, Massey University, Auckland, New Zealand.
Email: yiwen96@163.com

Funding information
Massey University Research Fund

Abstract
Using drones to monitor construction site is a flexible approach with low manpower costs. We study a drone scheduling problem in which a drone flies on a fixed path over a construction site. The flying speed of the drone is optimized to ensure that the drone spends the most time monitoring areas of the construction site that deserve the most attention while ensuring that the drone completes the route within a certain time and without depleting its battery. We propose a nonlinear optimization model for the problem and develop a dynamic programming algorithm to solve the model. A case study is carried out to demonstrate the applicability of the proposed drone scheduling model.

1 | INTRODUCTION

The construction industry is a labor-intensive industry with millions of employees working at construction sites. Despite an ancient industry, the construction industry has been always embracing new technologies that can increase efficiency, improve safety, and reduce costs. Drones are a technology that has aroused attention from a wide spectrum of industries in recent years. The construction industry is no exception: drones, equipped with video cameras, are frequently used in construction sites as an innovative technology. There are a number of benefits that can be reaped by using drones. First, drones provide real-time visual information of the progress of the project. For instance, the site manager will learn about information on the remaining amount of sand available in the site and the current volume of construction waste in the site. If the amount of sand is low, the manager will order more sand to be transported to the site; if the volume of construction waste is high, the manager will order trucks to transport the waste to disposal stations. Second, drones can monitor the safety of construction workers. A construction site is full of hazards because workers are often required to use large pieces of machinery and work at height. As a result, construction was among the industries with the most fatal injuries to workers (Collier, 2017). Using drones and imaging processing software packages (Nath, Behzadan, & Paal, 2020), the site manager can efficiently identify whether workers have complied with safety rules, for example, wearing helmets, vests, and not entering forbidden zones. For a large construction site, the tasks of checking the progress of the project and ensuring that workers have all complied with safety rules may take the manager or his delegate half a day, but a drone can complete the tasks in 10 min.

In almost all situations, drones are not allowed to fly autonomously, because they may hit buildings or moving objects such as tower cranes. In fact, it is a legal requirement in most countries that a drone used for commercial purposes must be operated by a professional with license, and the drone is required to remain within the operator's line of sight, so that the operator can look out for objects on the drone's route. Hence, the actual operating cost of a drone includes the manpower cost of the operator and is not as low as people may expect. Therefore, efficient scheduling of drones for construction site surveillance is of significant value for construction industry to use the technology in a cost-effective manner.

This study aims to develop models on drone scheduling for efficient construction site surveillance with a focus on optimizing the speed of the drone. It should be noted that the use of drone in construction is still in its infancy and the main issue has been the processing of information and integration with software in order for management to act. Therefore, the problem we address is of esoteric nature and is possibly ahead of its time. The area of drone scheduling for construction site surveillance is under-researched and we strongly believe that this is the next frontier to address.

1.1 | Literature review

The first type of relevant studies is deployment of sensors and video cameras to monitor an area. Chakrabarty, Iyengar, Qi, and Cho (2002) examined the problem of placement of sensors. They considered an area to monitor and different types of sensors, each of which has a detection range and cost. Their objective is to minimize the cost of sensors for complete coverage of the area. Morsly, Aouf, Djouadi, and Richardson (2012) examined a more general problem than that in Chakrabarty et al. (2002). They considered the placement of cameras considering the cameras' field of view. In a 2D space, the field of view of a camera is a fan that is related to the orientation of the camera, rather than a disk as in Chakrabarty et al. (2002). Mirchandani, Li, and Long (2010) addressed a radar locating problem and Altahir et al. (2017) addressed a camera locating problem for road sections, both similar to that of Morsly et al. (2012). Ai and Abouzeid (2006) addressed a problem similar to that of Morsly et al. (2012) except that Ai and Abouzeid (2006) aim to cover a set of discrete points, whereas Morsly et al. (2012) aim to cover a continuous area. Huang and Chang (2011) investigated the deployment of radio-frequency identification (RFID) tags. They modeled the coverage area of an RFID tag as an ellipse, whose direction of major axis is related to the direction of the antenna of the tag. Erdem and Sclaroff (2006) considered many practical features in surveillance using cameras, the most prominent one being the view of a camera may be blocked by objects. Murray, Kim, Davis, Machiraju, and Parent (2007) also took into account that the view of a camera may be blocked. X. Yang et al. (2018) calculated the Pareto-optimal solution for camera placement considering two objectives: maximizing coverage and minimizing cost, while taking into account cameras' field of view and visible region blockage. In all of the above studies, once a sensor/camera/RFID tag is deployed, the area that it can cover is fixed (cameras that can adjust orientations have some flexibility). By contrast, we focus on drone scheduling and drones can monitor a much larger area as they are mobile rather than fixed.

The second type of relevant studies is surveillance using drones with a focus on developing the technology that is suitable for certain application contexts (Otto, Agatz, Campbell, Golden, & Pesch, 2018; Rakha & Gorodetsky, 2018), such as construction structure health monitoring (Kang & Cha, 2018), construction structure displacement monitoring (Yoon, Shin, & Spencer, 2018), and bridge inspection (Omar & Nehdi, 2017; Seo, Duque, & Wacker, 2018). Cha, Choi, Suh, Mahmoudkhani, and Büyüköztürk (2018), F.C. Chen, Jahanshahi, Wu, and Joffe (2017), Yeum and Dyke (2015), and Liu, Nie, Fan, and Liu (2020) have developed techniques to analyze the images taken by drones to identify cracks in bridge structures. In this type of studies, the drone flies to a fixed point to take action at that point, and hence, in contrast to our study, these studies do not optimize the flying of the drones.

The third type of relevant studies is surveillance using drones with a focus on optimizing drone routes for monitoring a set of nodes, arcs, or areas. For instance, Xia, Wang, and Wang (2019) examined drone routing for monitoring air emissions from a set of vessels (nodes); Chow (2016) and Li, Zhen, Wang, Lv, and Qu (2018) have studied drone routing for monitoring vehicle traffic on a set of roads (arcs); Lim, Kim, Cho, Gong, and Khodaei (2016) proposed a drone prepositioning and routing model for power network damage assessment. Kim and Lim (2018) developed an algorithm for border surveillance using drones with an electrification line battery charging system. C.H. Yang, Tsai, Kang, and Hung (2018) studied the design of drone routes to monitor a region of debris fan (areas). Finally, it should be pointed out that the most prominent application of drones is cargo transportation (Otto et al., 2018). For instance, Kim, Lim, Cho, and Côté (2017) presented a model for delivering medicine to patients with chronic diseases in rural areas using drones. Kim, Lim, and Cho (2018) considered that the battery capacity of a drone depends on the air temperature, which is modeled as a random variable. Torabbeigi, Lim, and Kim (2019) further formulated a model taking into account that the battery consumption rate depends on the payload of drones. In all of the above studies, the flying speed of drones is fixed. By contrast, we focus on a drone scheduling problem in which drones can optimize their speed profiles to achieve utmost construction site surveillance effect.

1.2 | Objective

The objective of this research is to propose a drone scheduling model for effective construction site surveillance. We consider a drone that flies along a fixed path over a construction site and optimize the flying speed of the drone. The flying speed of the drone is optimized to ensure that the drone spends the most time monitoring areas of the construction site that deserve the most attention while

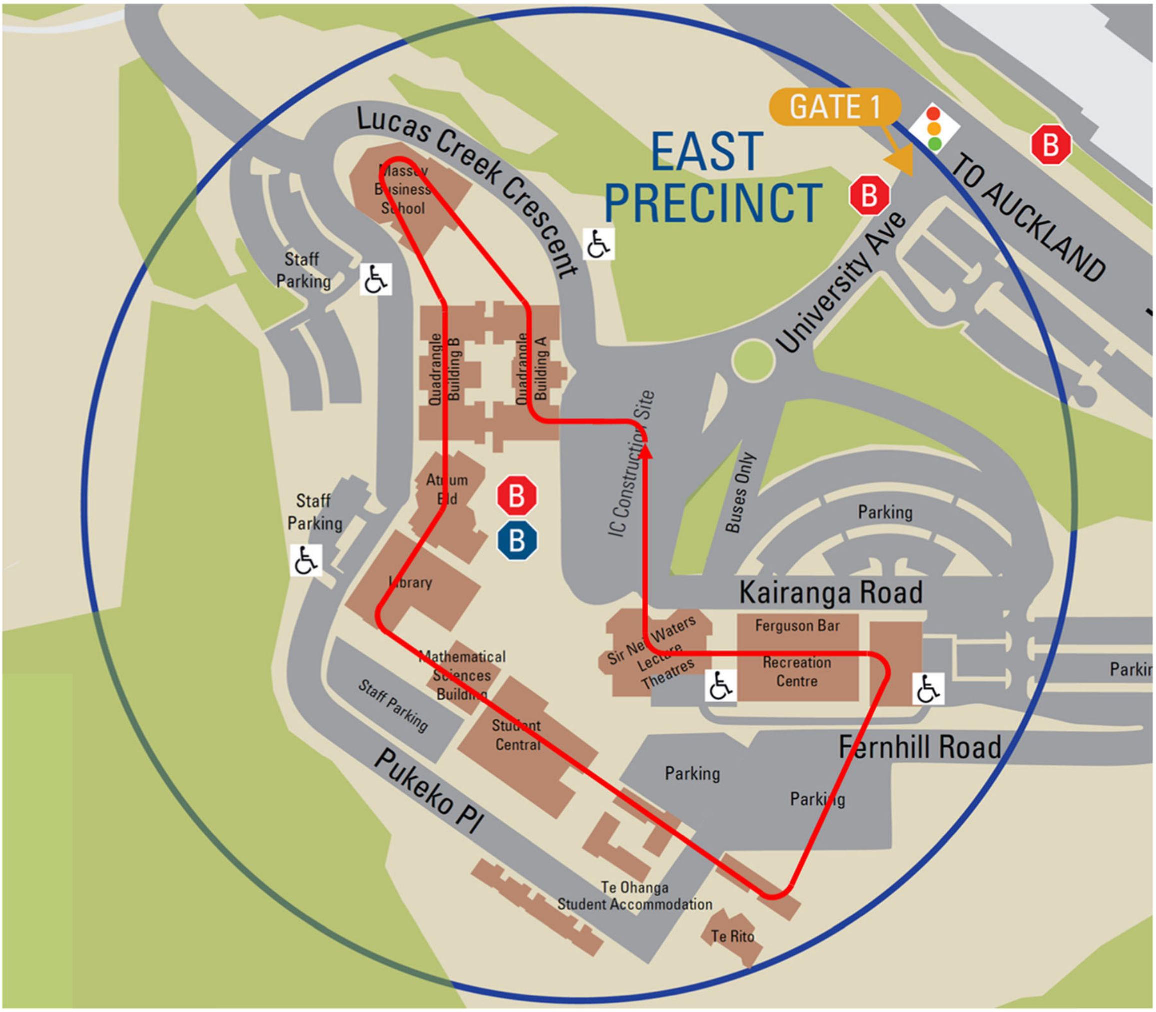

FIGURE 1 Flying route of the drone (red curve) for monitoring building construction and maintenance at Massey University

ensuring that the drone completes the route within a certain time and without depleting its battery.

The remainder of the paper is organized as follows: Section 2 presents the problem statement and model. Section 3 proposes the solution method. Section 4 reports the results of a case study. Section 5 concludes and discusses future research opportunities.

2 | PROBLEM DESCRIPTION AND MODEL

We consider a drone that monitors a construction site by flying along a fixed route, as shown in Figure 1. The drone must follow the route exactly. The length of the route is L (m). In general, the origin and the destination of the route are the same point, that is, the depot of the drone. It is required that the drone completes the route in time T (s). The minimum flying speed of the drone is $V^{\min}$ (m/s) and the maximum flying speed is $V^{\max}$ (m/s). The battery of the drone has an energy capacity of Q (J) and the energy consumption per meter (J/m) when the drone flies at the speed v (m/s) is denoted by $F(v)$, $V^{\min} \leq v \leq V^{\max}$. $F(v)$ is a nonlinear function and can be calibrated using measured data of speed and energy consumption.

The route can be divided into K segments, each of which represents an area of unique surveillance requirement such as a bar bending area, a material storage area, and a building that is being constructed or renovated. We further define the depot as segment 0. Define l_k as the distance from the origin of the route to the end of segment $k = 0, 1, \ldots, K$, $l_0 = 0$, and $l_K = L$. Then the length of segment $k = 1, \ldots, K$ is $l_k - l_{k-1}$. It is required that the minimum monitoring time of segment k is p_k, for example, the minimum monitoring time of a bar bending area is larger than that of a material storage area because the manager needs to pay more attention to the safety of workers in the bar bending area. When the actual monitoring time on segment k is larger than p_k, the site manager can have better understanding of the segment and hence there will be an additional surveillance benefit that is proportional to p_k. That is, if the actual monitoring time on segment k is t_k, then

$$\text{surveillance benefit} = \begin{cases} -\infty, & \text{if } t_k < p_k \\ p_k\left(t_k - p_k\right), & \text{otherwise.} \end{cases} \tag{1}$$

The drone may not be allowed to monitor a segment all the time. For instance, if tower cranes are working on a building, it is not safe to use the drone to monitor the building because the moving tower cranes may hit the drone. To take into account this factor, we define $[a_k, b_k]$ as the time window in which segment $k = 1, \ldots, K$ can be monitored. The drone must start to monitor the segment after a_k and finish monitoring the segment before b_k. If a segment k can be monitored all the time, for example, a storage location, we will set $a_k = 0$ and $b_k = T$. Moreover, because of different surveillance requirements for different segments, the drone does not fly at constant speed. We assume that the drone will accelerate or decelerate at the beginning of a segment to the regular speed and then fly at the regular speed until it arrives at the next segment. The acceleration of the drone will consume more energy than flying at a constant speed. To capture the energy consumed by acceleration, we denote by α (m/s^2) the acceleration and ρ_1 (W) the extra power required by acceleration. Similarly, we denote by $-\beta$ (m/s^2) the deceleration and ρ_2 (W) the reduced power during deceleration. $\alpha > 0,\ \beta > 0,\ \rho_1 > 0,\ \rho_2 > 0$.

The drone scheduling problem for construction site surveillance aims to determine the speed of the drone along the route to maximize the total surveillance benefit over all the segments while satisfying relevant constraints. We define the following decision variables.

Main decision variables:

- v_k: regular speed on segment k (the drone's speed after acceleration or deceleration at the beginning of segment k),
- t_k: flying time spent on segment k (including the acceleration or deceleration time and the regular speed flying time).

Auxiliary decision variables:

- T_k: arrival time at the end of segment $k = 0, 1, \ldots, K$; $T_0 = 0$,
- q_k^1: energy consumption during acceleration or deceleration on segment k,
- q_k^2: energy consumption during the flying at speed v_k on segment k.

The drone scheduling problem can be formulated as the following model:

[P]

$$\max \sum_{k=1}^{K} p_k\left(t_k - p_k\right) \tag{2}$$

subject to

$$t_k = \begin{cases} \dfrac{v_k - v_{k-1}}{\alpha} + \dfrac{l_k - l_{k-1} - \frac{(v_k)^2 - (v_{k-1})^2}{2\alpha}}{v_k}, & \text{if } v_k \geq v_{k-1} \\ \dfrac{v_k - v_{k-1}}{-\beta} + \dfrac{l_k - l_{k-1} - \frac{(v_k)^2 - (v_{k-1})^2}{-2\beta}}{v_k}, & \text{otherwise} \end{cases}, k = 1, \ldots, K, \tag{3}$$

$$t_k \geq p_k, k = 1, \ldots, K, \tag{4}$$

$$T_0 = 0, \tag{5}$$

$$T_k = T_{k-1} + t_k, k = 1, \ldots, K, \tag{6}$$

$$a_k \leq T_{k-1}, k = 1, \ldots, K, \tag{7}$$

$$T_k \leq b_k, k = 1, \ldots, K, \tag{8}$$

$$T_K \leq T, \tag{9}$$

$$v_0 = v_K, \tag{10}$$

$$q_k^1 = \begin{cases} \rho_1 \dfrac{v_k - v_{k-1}}{\alpha}, & \text{if } v_k \geq v_{k-1} \\ -\rho_2 \dfrac{v_k - v_{k-1}}{-\beta}, & \text{otherwise} \end{cases}, \quad k = 1, \ldots, K, \tag{11}$$

$$q_k^2 = \begin{cases} F\left(v_k\right)\left(l_k - l_{k-1} - \frac{(v_k)^2 - (v_{k-1})^2}{2\alpha}\right), & \text{if } v_k \geq v_{k-1} \\ F\left(v_k\right)\left(l_k - l_{k-1} - \frac{(v_k)^2 - (v_{k-1})^2}{-2\beta}\right), & \text{otherwise} \end{cases}, k = 1, \ldots, K, \tag{12}$$

$$\sum_{k=1}^{K}\left(q_k^1 + q_k^2\right) \leq Q, \tag{13}$$

$$V^{\min} \leq v_k \leq V^{\max},\ k = 1, \ldots, K. \tag{14}$$

The objective function (2) maximizes the total surveillance benefit over all the segments. Constraint (3) calculates the flying time on each segment taking into account acceleration and deceleration. Constraint (4) enforces that the flying time is larger than or equal to the minimum surveillance time required. Constraint (5) mandates that the departure time from segment 0 (i.e., the depot) is 0. Constraint (6) formulates the relation between the arrival time at the end of segment k and the arrival time at the end of segment $k-1$. Constraints (7) and (8) enforce time window constraints. Constraint (9) requires that the arrival time at the end of segment K does not exceed the maximum flying time T. Constraint (10) requires that the regular speed on segment 0 and the regular speed on segment K are the same. This constraint ensures that the drone can fly repeatedly on the route to monitor the construction site. Constraint (11) calculates the energy consumed due to acceleration and deceleration. Constraint (12) calculates the energy consumed during regular flying time. Constraint (13) stipulates that the total energy consumption for the drone to complete the route is at most Q. Constraint (14) specifies the lower and upper bounds of the flying speeds on the route.

3 | SOLUTION METHOD

Model [P] is challenging to solve because it has complex nonlinear constraints (3) and (12) and cannot be solved by off-the-shelf solvers (Adeli & Karim, 2014; García-Nieves, Ponz-Tienda, Salcedo-Bernal, & Pellicer, 2018; Jiang & Adeli, 2003; Tang, Liu, Wang, Sun, & Kandil, 2018; Wang, Yan, & Qu, 2019; Xie, Lei, & Ouyang, 2018). One approach is to apply nonlinear optimization methods (Arcaro & Adeli, 2019; Bie, Xiong, Yan, & Qu, 2020; Z. Chen & Liu, 2019; Pu et al., 2019; Qu, Yu, Zhou, Lin, & Wang, 2020; Zavadskas, Antucheviciene, Turskis, & Adeli, 2016; Zavadskas, Antucheviciene, Vilutiene, & Adeli, 2018; Zhang et al., 2019; Zhou, Yu, & Qu, 2020), such as Newton method or quasi-Newton method (Branam, Arcaro, & Adeli, 2019), but they do not guarantee global optimality. Another approach is to use metaheuristics, such as neural networks (Adeli & Karim, 1997; Rokibul Alam, Siddique, & Adeli, 2019), spider monkey optimization (Akhand, Ayon, Shahriyar, Siddique, & Adeli, 2020), and particle swarm optimization (Hossain, Akhand, Shuvo, Siddique, & Adeli, 2019), but these methods do not even guarantee local optimality. A final approach is to develop tailored methods (Meng, Wang, & Lee, 2015; Wang, Zhang, & Qu, 2018), and we adopt this approach.

To address the challenges, we examine the properties of the problem and develop a tailored solution method. In particular, the problem has a nice "history-independent" property: the optimal speed decision for a segment k depends only on the speed at the beginning of segment k (i.e., the regular speed on segment $k-1$), the total consumed energy on segments $1, \ldots, k-1$, and the total flying time on segments $1, \ldots, k-1$, but not the detailed allocation of flying time on each of the segments $1, \ldots, k-1$. We can therefore develop a dynamic-programming-based approach to solve the problem.

To apply the dynamic programming based approach, we divide the battery energy, flying time, and flying speed into discrete values. To simplify the notation, we use appropriate units for battery energy, flying time, and flying speed, and then, discretize them into integer values. Denote by Q_k the total used energy consumed over segments $1, \ldots, k$. Recall that T_k and v_k are the total flying time over segments $1, \ldots, k$ and regular speed at the end of segment $k = 1, \ldots, K$, respectively. We enumerate all possible value of $v_0 = V^{\min}, \ldots, V^{\max}$, which are also the regular speed on segment K. Define $V_k(v_0, Q_{k-1}, T_{k-1}, v_{k-1})$ as the highest total surveillance benefit over segments $k, k+1, \ldots, K$, given the system state is $(v_0, Q_{k-1}, T_{k-1}, v_{k-1})$ when the drone arrives at the end of segment $k-1$. Note that we have parameter v_0 in $V_k(v_0, Q_{k-1}, T_{k-1}, v_{k-1})$ because it dictates v_K, as shown in Equation (10). Denote by $v_k^*(v_0, Q_{k-1}, T_{k-1}, v_{k-1})$ the optimal regular speed for segment k, given the system state is $(v_0, Q_{k-1}, T_{k-1}, v_{k-1})$, and then, for $k = 1, \ldots, K-1$, $v_k^*(v_0, Q_{k-1}, T_{k-1}, v_{k-1})$ is the optimal solution to the following model:

$$V_k\left(v_0, Q_{k-1}, T_{k-1}, v_{k-1}\right) = \max_{v_k} \left[p_k\left(t_k - p_k\right) + V_{k+1}\left(v_0, Q_k, T_k, v_k\right)\right] \tag{15}$$

subject to

$$v_k = V^{\min}, \ldots, V^{\max}, \tag{16}$$

$$t_k = \begin{cases} \frac{v_k - v_{k-1}}{\alpha} + \frac{l_k - l_{k-1} - \frac{(v_k)^2 - (v_{k-1})^2}{2\alpha}}{v_k}, & \text{if } v_k \geq v_{k-1} \\ \frac{v_k - v_{k-1}}{-\beta} + \frac{l_k - l_{k-1} - \frac{(v_k)^2 - (v_{k-1})^2}{-2\beta}}{v_k}, & \text{otherwise} \end{cases}, \tag{17}$$

$$t_k \geq p_k, \tag{18}$$

$$T_k = T_{k-1} + t_k, \tag{19}$$

$$a_{k+1} \leq T_k \leq b_k, \tag{20}$$

$$q_k^1 = \begin{cases} \rho_1 \frac{v_k - v_{k-1}}{\alpha}, & \text{if } v_k \geq v_{k-1} \\ -\rho_2 \frac{v_k - v_{k-1}}{-\beta}, & \text{otherwise} \end{cases}, \tag{21}$$

$$q_k^2 = \begin{cases} F(v_k)\left(l_k - l_{k-1} - \frac{(v_k)^2 - (v_{k-1})^2}{2\alpha}\right), & \text{if } v_k \geq v_{k-1} \\ F(v_k)\left(l_k - l_{k-1} - \frac{(v_k)^2 - (v_{k-1})^2}{-2\beta}\right), & \text{otherwise} \end{cases}, \tag{22}$$

$$Q_k = Q_{k-1} + q_k^1 + q_k^2. \tag{23}$$

For $k = K$, if $v_K = v_0$ is a feasible solution to the following model (24), then $v_K^*(v_0, Q_{K-1}, T_{K-1}, v_{K-1}) = v_0$; otherwise, there is no feasible solution:

$$V_K(v_0, Q_{K-1}, T_{K-1}, v_{K-1}) = \max_{v_K} p_K (t_K - p_K) \tag{24}$$

subject to

$$v_K = v_0, \tag{25}$$

$$t_K = \begin{cases} \frac{v_K - v_{K-1}}{\alpha} + \frac{l_K - l_{K-1} - \frac{(v_K)^2 - (v_{K-1})^2}{2\alpha}}{v_K}, & \text{if } v_K \geq v_{K-1} \\ \frac{v_K - v_{K-1}}{-\beta} + \frac{l_K - l_{K-1} - \frac{(v_K)^2 - (v_{K-1})^2}{-2\beta}}{v_K}, & \text{otherwise} \end{cases}, \tag{26}$$

$$t_K \geq p_K, \tag{27}$$

$$T_K = T_{K-1} + t_K, \tag{28}$$

$$T_K \leq b_K, \tag{29}$$

$$T_K \leq T, \tag{30}$$

$$q_K^1 = \begin{cases} \rho_1 \frac{v_K - v_{K-1}}{\alpha}, & \text{if } v_K \geq v_{K-1} \\ -\rho_2 \frac{v_K - v_{K-1}}{-\beta}, & \text{otherwise} \end{cases}, \tag{31}$$

$$q_K^2 = \begin{cases} F(v_K)\left(l_K - l_{K-1} - \frac{(v_K)^2 - (v_{K-1})^2}{2\alpha}\right), & \text{if } v_K \geq v_{K-1} \\ F(v_K)\left(l_K - l_{K-1} - \frac{(v_K)^2 - (v_{K-1})^2}{-2\beta}\right), & \text{otherwise} \end{cases}, \tag{32}$$

$$Q_K = Q_{K-1} + q_K^1 + q_K^2, \tag{33}$$

$$Q_K \leq Q. \tag{34}$$

Having calculated all the values of $V_k(v_0, Q_{k-1}, T_{k-1}, v_{k-1})$, $k = 1, \ldots, K$, $v_0 = V^{\min}, \ldots, V^{\max}$, $Q_{k-1} = 0, \ldots, Q$, $T_{k-1} = 0, \ldots, T$, $v_{k-1} = V^{\min}, \ldots, V^{\max}$, we eventually need to solve the following problem:

$$\max_{v_0 = V^{\min}, \ldots, V^{\max}, T_0 = 0} V_1(v_0, Q, T_0, v_0). \tag{35}$$

The optimal speed on each segment is available in the solution of the above models.

The overall algorithm is summarized in Algorithm 1.

***Algorithm 1**. Dynamic programming for drone scheduling*

For each v_0 in $V^{\min}, \ldots, V^{\max}$:
  For each k in $K, \ldots, 1$:
  If $k = K$, enumerate all possible values of Q_{k-1}, T_{k-1}, and v_{k-1}. In particular, $Q_{k-1} = 0, 1, \ldots, Q$, $T_{k-1} = 0, 1, \ldots, T$, and $v_{k-1} = V^{\min}, \ldots, V^{\max}$. For each $(v_0, Q_{k-1}, T_{k-1}, v_{k-1})$, solve model (24) to obtain $V_k(v_0, Q_{k-1}, T_{k-1}, v_{k-1})$.
  If $k = K - 1, \ldots, 1$, enumerate all possible values of Q_{k-1}, T_{k-1}, and v_{k-1}. In particular, $Q_{k-1} = 0, 1, \ldots, Q$, $T_{k-1} = 0, 1, \ldots, T$, and $v_{k-1} = V^{\min}, \ldots, V^{\max}$. For each $(v_0, Q_{k-1}, T_{k-1}, v_{k-1})$, solve model (15) to obtain $V_k(v_0, Q_{k-1}, T_{k-1}, v_{k-1})$.
  Solve model (35) to obtain the largest total surveillance benefit and the resulting optimal speed decisions.

It can be easily seen in the following proposition.

Proposition 1. *Algorithm 1 terminates in time bounded by* $O(KQT(V^{\max})^3)$.

Hence, Algorithm 1 is pseudopolynomial in time complexity.

4 | COMPUTATIONAL EXPERIMENTS

We carry out a case study to demonstrate the applicability of the proposed model and algorithm. The case study is on the construction of Innovation Complex (IC) and the renovation of existing buildings near Gate 1 of Massey University, as shown in Figure 1. The route of the drone is divided into 16 segments, whose lengths and minimum monitoring time are shown in Table 1. Segment 1 is the IC construction site and requires the most surveillance attention. Segment 8 is the library, which needs extensive renovation work, and it also requires significant surveillance attention. Segments 4, 11, 15, and 16 also require significant surveillance attention.

The drone is a DJI P4 PRO. Table 2 shows its flying duration and flying distance at different speeds. It can be seen

TABLE 1 Information of the 16 segments on the route

Segment	Length (m)	Minimum monitoring time (s)	Note
1	115	18	Innovation Complex (IC) construction site
2	70	6	Quadrangle Building A
3	63	0	Lawn
4	94	7	Massey Business School
5	31	0	Lawn
6	71	6	Quadrangle Building B
7	60	5	Atrium Building
8	64	8	Library
9	30	0	Lawn
10	25	2	Mathematical Science Building
11	87	7	Student Central
12	55	4	Te Ohanga
13	44	4	Te Rito
14	109	0	Parking
15	112	9	Recreation Center
16	90	7	Sir Neil Waters Lecture Theatres

TABLE 2 Information on the drone DJI P4 PRO

Flying speed (km/hr)	Flying duration (min)	Flying distance (km)
5	28	2.3
10	27.5	4.6
15	27	6.8
20	25.5	8.5
25	24	10.0
30	23	11.5
35	22	12.8
40	20	13.3

Source: Steiner (2017).

that $F(v)$ is smaller when v is larger. In our case study, we set $V^{\min} = 2$ m/s, $V^{\max} = 11$ m/s, and the total amount of battery energy as 100 units but the battery needs to sustain four trips (the drone will replace its battery after completing four trips). Hence, the total amount of energy that can be used is 25 units. The acceleration is 2 m/s^2 and the deceleration is 3 m/s^2. The extra amount of energy consumed during acceleration is 0.08 unit/s and the amount of energy saved during deceleration is 0.03 unit/s.

TABLE 3 Optimal solution

Segment	Optimal flying time t_k (s)	Optimal flying speed v_k (m/s)
1	57	2
2	10	8
3	6	11
4	9	11
5	3	11
6	7	11
7	6	10
8	12	5
9	4	9
10	3	10
11	8	11
12	5	11
13	4	11
14	10	11
15	18	6
16	18	5

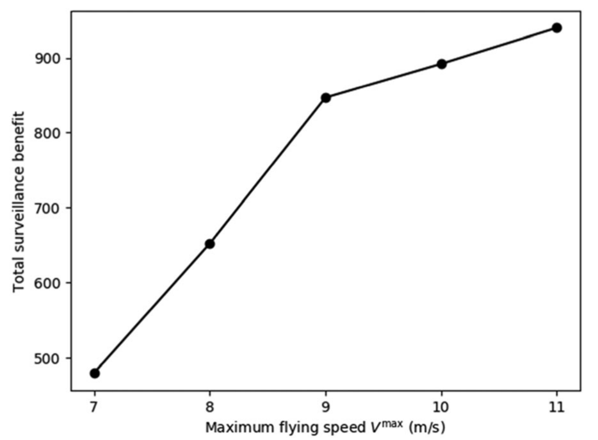

FIGURE 2 Sensitivity of the total surveillance benefit in the maximum flying speed

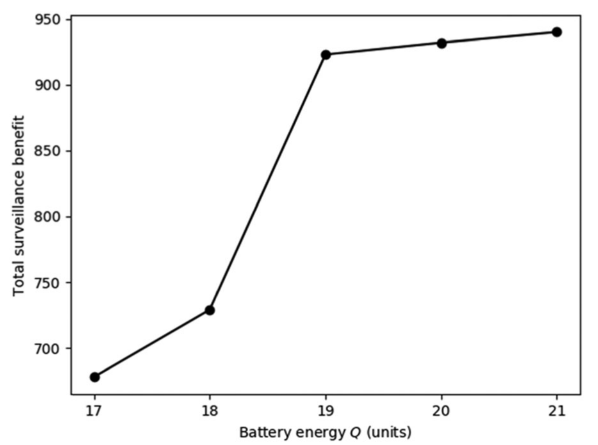

FIGURE 3 Sensitivity of the total surveillance benefit in the battery energy

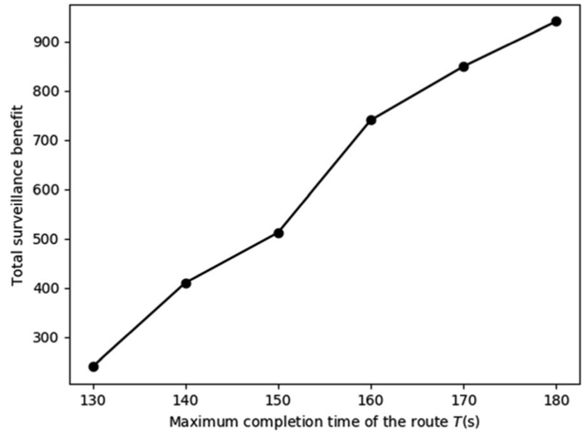

FIGURE 4 Sensitivity of the total surveillance benefit in the maximum completion time of the route

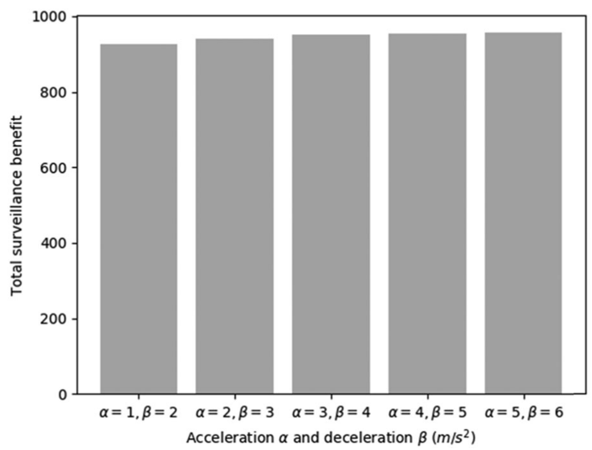

FIGURE 5 Sensitivity of the total surveillance benefit in the acceleration/deceleration of the drone

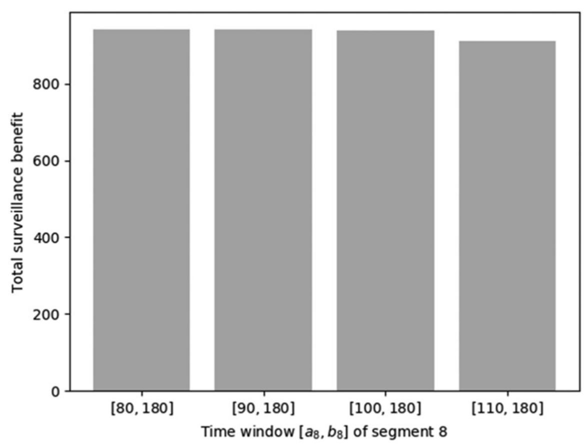

FIGURE 6 Sensitivity of the total surveillance benefit in the time window

The drone needs to complete the route in $T = 180$ s. The time windows for all segments are $[0, T]$. The dynamic programming algorithm is coded in Python and run on a PC equipped with 3.60 GHz of Intel Core i7 CPU and 16GB of RAM.

The optimal total surveillance effect for the above base case is 940. In the optimal solution, the total flying time is exactly 180 s (constraint (9) is binding), and the total amount of energy used is 21 units (constraint (13) is unbinding).

The optimal solutions of t_k and v_k are shown in Table 3. We can see from Table 3 that the solution has a clear structure. Segment 1 (IC construction site) requires the most surveillance efforts and its optimal speed is the lowest (2 m/s). Segment 8 has very low speed (5 m/s) because it also requires significant surveillance attention. The speeds of the drone on segments 15 and 16 are low because on the one side, they require significant surveillance attention and on the other side the drone needs to slow down before arriving at segment 1, which requires the most surveillance efforts. The speeds on segments 4 and 11 are high because their neighboring segments (segments 3, 5, 10, and 12) require low or no surveillance attention and the total surveillance time limit does not allow the drone to decelerate and accelerate frequently.

The sensitivity of the total surveillance effect in the maximum flying speed is plotted in Figure 2. It can be seen that as the maximum flying speed increases, the total surveillance effect increases monotonically. Moreover, the marginal benefit of increasing the maximum flying speed decreases with the maximum flying speed. This has the managerial implication that designing drones with extremely high speeds may not be of much value for surveillance purposes (of course, they may have value for transportation).

The sensitivity of the total surveillance effect in the capacity of the battery is plotted in Figure 3. It can be seen that as the capacity of the battery increases, the total surveillance benefit increases monotonically, but not convexly or concavely. Therefore, whether the marginal benefit of using a battery of more energy justifies its higher cost has to be analyzed on a case-by-case basis.

The sensitivity of the total surveillance effect in the maximum completion time of the route is plotted in Figure 4. It can be seen that as the maximum completion time of the route increases, the total surveillance benefit increases monotonically. Moreover, the total surveillance benefit is very sensitive to the maximum completion time of the route.

The sensitivity of the total surveillance effect in the acceleration/deceleration of the drone is plotted in Figure 5. It can be seen that as the acceleration/deceleration capability of the drone increases, the total surveillance

TABLE 4 Comparison between the heuristic and the dynamic programming algorithm

Total surveillance benefit	Heuristic	Dynamic programming	Improvement
Base case	175	940	437%
$V^{\max} = 10$	230	892	288%
$V^{\max} = 9$	296	847	186%
$V^{\max} = 8$	379	652	72%
$V^{\max} = 7$	433	479	11%
$Q = 20$	175	932	433%
$Q = 19$	175	923	427%
$Q = 18$	175	729	317%
$Q = 17$	175	678	287%
$T = 170$	175	849	385%
$T = 160$	175	740	323%
$T = 150$	175	512	193%
$T = 140$	175	410	134%
$T = 130$	171	240	40%
$\alpha = 1, \beta = 2$	170	928	446%
$\alpha = 3, \beta = 4$	178	951	434%
$\alpha = 4, \beta = 5$	180	954	430%
$\alpha = 5, \beta = 6$	181	956	428%
$[a_8, b_8] = [80, 180]$	No feasible solution found	940	NA
$[a_8, b_8] = [90, 180]$	No feasible solution found	940	NA
$[a_8, b_8] = [100, 180]$	No feasible solution found	937	NA
$[a_8, b_8] = [110, 180]$	No feasible solution found	912	NA

benefit increases slightly. In other words, the total surveillance effect is hardly sensitive to the acceleration/deceleration of the drone.

The sensitivity of the total surveillance effect in the time window of segment 8 is plotted in Figure 6. It can be seen that as the time window is tighter, the total surveillance benefit decreases monotonically. It should be noted that when the time window is [120, 180], no feasible solution exists.

We benchmark the performance of the dynamic programming algorithm with a heuristic. The heuristic works as follows: for each segment k, we calculate its maximum allowed speed μ_k that is equal to $V^{\max}$ if $p_k = 0$ and $\min\{V^{\max}, (l_k - l_{k-1})/p_k\}$ otherwise. We then allow the regular speed for each segment k to take a value from μ_k, $\min(V^{\max}, \mu_k + 1)$, and $\max(V^{\min}, \mu_k - 1)$. Among all the possible combinations of the speeds on the K segments, we identify the one that performs the best. We recalculate all the above cases using the heuristic, and the comparison with the dynamic programming algorithm is shown in Table 4. The table clearly demonstrates the superiority of the proposed dynamic programming method. Without considering the cases for which the heuristic does not return a feasible solution, the average improvement of the dynamic programming method over the heuristic is 293%. Considering that average hourly rate of drone use in construction is \$168 (Drone Deploy, 2017), the approximate costing savings of optimizing the speed can be $\$168/\mathrm{hr}/(1 + 293\%) = \$125/\mathrm{hr}$.

5 | CONCLUSIONS AND FUTURE WORK

This study has proposed a drone scheduling problem in which a drone flies on a fixed path over a construction site. The flying speed of the drone is optimized to ensure that the drone spends the most time monitoring areas of the construction site that are worth the most attention while ensuring that the drone completes the route within a certain time and without depleting its battery. We propose a dynamic programming algorithm to solve the problem. A case study is carried out to demonstrate the applicability of the proposed drone scheduling model. The numerical results show that the optimal flying speed on a segment depends not only on its own minimum surveillance requirement but also on its neighboring segments' minimum surveillance requirements. Moreover, we find that the total surveillance benefit is very sensitive to the maximum flying speed, the battery energy, and the maximum completion time of the route, but hardly sensitive to the acceleration/deceleration of the drone. We have further compared the dynamic programming algorithm with a heuristic, and the results clearly demonstrate the superiority of the proposed dynamic programming method.

The extensive numerical experiments have confirmed that the proposed model is correctly implemented, that is, it matches the specifications and assumptions for the drone scheduling application. Still, the validation of the model, that is, checking the accuracy of the model's representation of the real system, should be carried out in field studies.

Our model has implicitly considered the effect the obstacles and movement of elements. That is, the design of the flying route should avoid obstacles and movement of elements. Since construction sites are open air, drones cannot be used in adverse weather conditions, for example, strong wind and heavy rain.

Our model is most useful when the situation of the construction site frequently changes. This is usually the case for prefab construction, that is, construction using prefabricated modules in factories (e.g., bathroom modules, stairway models, and walls). Prefab construction is very efficient, for instance, one floor of a building can be constructed in 3 days. With such a rapid pace, the fixed facilities and temporary facilities of the construction site will frequently change and an automated decision support system for drone scheduling will be of great help.

We will explore two future research directions. The first one is scheduling multiple drones for monitoring one construction site. The second one is jointly routing and scheduling drones for effective surveillance of construction site.

ACKNOWLEDGMENT

This study is supported by Massey University Research Fund.

REFERENCES

Adeli, H., & Karim, A. (1997). Scheduling/cost optimization and neural dynamics model for construction. *Journal of Construction Engineering and Management*, *123*(4), 450–458.

Adeli, H., & Karim, A. (2014). *Construction scheduling, cost optimization and management*. Boca Raton, FL: CRC Press.

Ai, J., & Abouzeid, A. A. (2006). Coverage by directional sensors in randomly deployed wireless sensor networks. *Journal of Combinatorial Optimization*, *11*(1), 21–41.

Akhand, M. A. H., Ayon, S. I., Shahriyar, S. A., Siddique, N., & Adeli, H. (2020). Discrete spider monkey optimization for traveling salesman problem. *Applied Soft Computing*, *86*, 105887.

Altahir, A. A., Asirvadam, V. S., Hamid, N. H., Sebastian, P., Saad, N., Ibrahim, R., & Dass, S. C. (2017). Modeling multicamera coverage for placement optimization. *IEEE Sensors Letters*, *1*(6), 1–4.

Arcaro, V., & Adeli, H. (2019). Form-finding and analysis of hyperelastic tensegrity structures using unconstrained nonlinear programming. *Engineering Structures*, *191*, 439–446.

Bie, Y., Xiong, X., Yan, Y., & Qu, X. (2020). Dynamic headway control for high-frequency bus line based on speed guidance and intersection signal adjustment. *Computer-Aided Civil and Infrastructure Engineering*, *35*(1), 4–25.

Branam, N. J., Arcaro, V., & Adeli, H. (2019). A unified approach for analysis of cable and tensegrity structures using memoryless quasi-Newton minimization of total strain energy. *Engineering Structures*, *179*, 332–340.

Cha, Y. J., Choi, W., Suh, G., Mahmoudkhani, S., & Büyüköztürk, O. (2018). Autonomous structural visual inspection using region-based deep learning for detecting multiple damage types. *Computer-Aided Civil and Infrastructure Engineering*, *33*(9), 731–747.

Chakrabarty, K., Iyengar, S. S., Qi, H., & Cho, E. (2002). Grid coverage for surveillance and target location in distributed sensor networks. *IEEE Transactions on Computers*, *51*(12), 1448–1453.

Chen, F. C., Jahanshahi, M. R., Wu, R. T., & Joffe, C. (2017). A texture-based video processing methodology using Bayesian data fusion for autonomous crack detection on metallic surfaces. *Computer-Aided Civil and Infrastructure Engineering*, *32*(4), 271–287.

Chen, Z., & Liu, X. C. (2019). Roadway asset inspection sampling using high-dimensional clustering and locality-sensitivity hashing. *Computer-Aided Civil and Infrastructure Engineering*, *34*(2), 116–129.

Chow, J. Y. (2016). Dynamic UAV-based traffic monitoring under uncertainty as a stochastic arc-inventory routing policy. *International Journal of Transportation Science and Technology*, *5*(3), 167–185.

Collier, E. (2017). Ten common construction site hazards. Retrieved from https://www.highspeedtraining.co.uk/hub/common-construction-hazards/

Drone Deploy. (2017). How to price your drone mapping services. Retrieved from https://medium.com/aerial-acuity/how-to-price-your-drone-mapping-services-b5fc31c86934

Erdem, U. M., & Sclaroff, S. (2006). Automated camera layout to satisfy task-specific and floor plan-specific coverage requirements. *Computer Vision and Image Understanding*, *103*(3), 156–169.

García-Nieves, J. D., Ponz-Tienda, J. L., Salcedo-Bernal, A., & Pellicer, E. (2018). The multimode resource-constrained project scheduling problem for repetitive activities in construction projects. *Computer-Aided Civil and Infrastructure Engineering*, *33*(8), 655–671.

Hossain, S. I., Akhand, M. A. H., Shuvo, M. I. R., Siddique, N., & Adeli, H. (2019). Optimization of university course scheduling problem using particle swarm optimization with selective search. *Expert Systems with Applications*, *127*, 9–24.

Huang, H. P., & Chang, Y. T. (2011). Optimal layout and deployment for RFID systems. *Advanced Engineering Informatics*, *25*(1), 4–10.

Jiang, X., & Adeli, H. (2003). Freeway work zone traffic delay and cost optimization model. *Journal of Transportation Engineering*, *129*(3), 230–241.

Kang, D., & Cha, Y. J. (2018). Autonomous UAVs for structural health monitoring using deep learning and an ultrasonic beacon system with geo-tagging. *Computer-Aided Civil and Infrastructure Engineering*, *33*(10), 885–902.

Kim, S. J., & Lim, G. J. (2018). Drone-aided border surveillance with an electrification line battery charging system. *Journal of Intelligent & Robotic Systems*, *92*(3–4), 657–670.

Kim, S. J., Lim, G. J., & Cho, J. (2018). Drone flight scheduling under uncertainty on battery duration and air temperature. *Computers & Industrial Engineering*, *117*, 291–302.

Kim, S. J., Lim, G. J., Cho, J., & Côté, M. J. (2017). Drone-aided healthcare services for patients with chronic diseases in rural areas. *Journal of Intelligent & Robotic Systems*, *88*(1), 163–180.

Li, M., Zhen, L., Wang, S., Lv, W., & Qu, X. (2018). Unmanned aerial vehicle scheduling problem for traffic monitoring. *Computers & Industrial Engineering*, *122*, 15–23.

Lim, G. J., Kim, S., Cho, J., Gong, Y., & Khodaei, A. (2016). Multi-UAV pre-positioning and routing for power network damage assessment. *IEEE Transactions on Smart Grid*, *9*(4), 3643–3651.

Liu, Y. F., Nie, X., Fan, J. S., & Liu, X. G. (2020). Image-based crack assessment of bridge piers using unmanned aerial vehicles and three-dimensional scene reconstruction. *Computer-Aided Civil and Infrastructure Engineering*, *35*, 511–529. https://doi.org/10.1111/mice.12501.

Meng, Q., Wang, S., & Lee, C. Y. (2015). A tailored branch-and-price approach for a joint tramp ship routing and bunkering problem. *Transportation Research Part B: Methodological*, *72*, 1–19.

Mirchandani, P. B., Li, J. Q., & Long, Y. (2010). Locating a surveillance infrastructure in and near ports or on other planar surfaces to monitor flows. *Computer-Aided Civil and Infrastructure Engineering*, *25*(2), 89–100.

Morsly, Y., Aouf, N., Djouadi, M. S., & Richardson, M. (2012). Particle swarm optimization inspired probability algorithm for optimal camera network placement. *IEEE Sensors Journal*, *12*(5), 1402–1412.

Murray, A. T., Kim, K., Davis, J. W., Machiraju, R., & Parent, R. (2007). Coverage optimization to support security monitoring. *Computers, Environment and Urban Systems*, *31*(2), 133–147.

Nath, N. D., Behzadan, A. H., & Paal, S. G. (2020). Deep learning for site safety: Real-time detection of personal protective equipment. *Automation in Construction*, *112*, 103085.

Omar, T., & Nehdi, M. L. (2017). Remote sensing of concrete bridge decks using unmanned aerial vehicle infrared thermography. *Automation in Construction*, *83*, 360–371.

Otto, A., Agatz, N., Campbell, J., Golden, B., & Pesch, E. (2018). Optimization approaches for civil applications of unmanned aerial vehicles (UAVs) or aerial drones: A survey. *Networks*, *72*(4), 411–458.

Pu, H., Song, T., Schonfeld, P., Li, W., Zhang, H., Wang, J., … Peng, X. (2019). A three-dimensional distance transform for optimizing constrained mountain railway alignments. *Computer-Aided Civil and Infrastructure Engineering*, *34*, 372–990. https://doi.org/10.1111/mice.12475.

Qu, X., Yu, Y., Zhou, M., Lin, C. T., & Wang, X. (2020). Jointly dampening traffic oscillations and improving energy consumption with electric, connected and automated vehicles: A reinforcement learning based approach. *Applied Energy*, *257*, 114030.

Rakha, T., & Gorodetsky, A. (2018). Review of unmanned aerial system (UAS) applications in the built environment: Towards automated building inspection procedures using drones. *Automation in Construction*, *93*, 252–264.

Rokibul Alam, K. M., Siddique, N., & Adeli, H. (2019). A dynamic ensemble learning algorithm for neural networks. *Neural Computing and Applications*, https://doi.org/10.1007/s00521-019-04359-7.

Seo, J., Duque, L., & Wacker, J. (2018). Drone-enabled bridge inspection methodology and application. *Automation in Construction*, *94*, 112–126.

Steiner, E. (2017). Drone flight stats. Retrieved from https://airdata.com/blog/2017/drone-flight-stats-part-1

Tang, Y., Liu, R., Wang, F., Sun, Q., & Kandil, A. A. (2018). Scheduling optimization of linear schedule with constraint programming. *Computer-Aided Civil and Infrastructure Engineering*, *33*(2), 124–151.

Torabbeigi, M., Lim, G. J., & Kim, S. J. (2019). Drone delivery scheduling optimization considering payload-induced battery consumption rates. *Journal of Intelligent & Robotic Systems*, *1*, 1–17.

Wang, S., Yan, R., & Qu, X. (2019). Development of a non-parametric classifier: Effective identification, algorithm, and applications in port state control for maritime transportation. *Transportation Research Part B: Methodological*, *128*, 129–157.

Wang, S., Zhang, W., & Qu, X. (2018). Trial-and-error train fare design scheme for addressing boarding/alighting congestion at CBD stations. *Transportation Research Part B: Methodological*, *118*, 318–335.

Xia, J., Wang, K., & Wang, S. (2019). Drone scheduling to monitor vessels in emission control areas. *Transportation Research Part B: Methodological*, *119*, 174–196.

Xie, S., Lei, C., & Ouyang, Y. (2018). A customized hybrid approach to infrastructure maintenance scheduling in railroad networks under variable productivities. *Computer-Aided Civil and Infrastructure Engineering*, *33*(10), 815–832.

Yang, C. H., Tsai, M. H., Kang, S. C., & Hung, C. Y. (2018). UAV path planning method for digital terrain model reconstruction—A debris fan example. *Automation in Construction*, *93*, 214–230.

Yang, X., Li, H., Huang, T., Zhai, X., Wang, F., & Wang, C. (2018). Computer-aided optimization of surveillance cameras placement on construction sites. *Computer-Aided Civil and Infrastructure Engineering*, *33*(12), 1110–1126.

Yeum, C. M., & Dyke, S. J. (2015). Vision-based automated crack detection for bridge inspection. *Computer-Aided Civil and Infrastructure Engineering*, *30*(10), 759–770.

Yoon, H., Shin, J., & Spencer, B. F. (2018). Structural displacement measurement using an unmanned aerial system. *Computer-Aided Civil and Infrastructure Engineering*, *33*(3), 183–192.

Zavadskas, E. K., Antucheviciene, J., Turskis, Z., & Adeli, H. (2016). Hybrid multiple-criteria decision-making methods: A review of applications in engineering. *Scientia Iranica. Transaction A, Civil Engineering*, *23*(1), 1–20.

Zavadskas, E. K., Antucheviciene, J., Vilutiene, T., & Adeli, H. (2018). Sustainable decision-making in civil engineering, construction and building technology. *Sustainability*, *10*(1), 14–34.

Zhang, A., Wang, K. C., Fei, Y., Liu, Y., Chen, C., Yang, G., … Qiu, S. (2019). Automated pixel-level pavement crack detection on 3D asphalt surfaces with a recurrent neural network. *Computer-Aided Civil and Infrastructure Engineering*, *34*(3), 213–229.

Zhou, M., Yu, Y., & Qu, X. (2020). Development of an efficient driving strategy for connected and automated vehicles at signalized intersections: A reinforcement learning approach. *IEEE Transactions on Intelligent Transportation Systems*, *21*(1), 433–443.

How to cite this article: Yi W, Sutrisna M. Drone scheduling for construction site surveillance. *Comput Aided Civ Inf*. 2021;36:3–13. https://doi.org/10.1111/mice.12593